

# Erosion of metal plasma facing components by arcing at the inner divertor baffle of ASDEX Upgrade

V.Rohde, M.Balden, and the ASDEX Upgrade Team

*Max Planck Institut für Plasmaphysik, Boltzmannstr. 2, 85478 Garching, Germany*

## INTRODUCTION:

In the standard picture of plasma wall interaction (PWI) arcs are not taken into account as erosion source: in the 80<sup>th</sup> it was shown that for carbon physical and chemical sputtering dominate and arcs are only triggered during unstable plasma phases [1]. On the other hand arc traces are observed in all present fusion devices. Recently, investigations in ASDEX Upgrade (AUG) show that ELMs may trigger arcs at some locations [2] and the morphology of dust collected can be explained by droplet production in arcs [3].

Whereas previous investigations use the typical AUG PFCs, i.e. tungsten (W) coating of 5 micron thickness on a carbon substrate, bulk material was investigated this time. Polished probes were used as the surface roughness of technical materials is in the micron range, which is the typical width of arc traces. Moreover, scratches produced during the fabrication process influence the direction of arcs and even hide them. Two different materials were selected: W as material of the ITER divertor and P92, martensitic-ferritic high temperature steel similar to EUROFER, which is under discussion for DEMO.

## ARCING:

In contrast to sputter processes, arcs are localized and the amount of arc traces varies strongly locally even on a single tile. Markers, made out of polished W and P92 steel, were installed at the inner divertor baffle region, which is prone for arcing [2, 4] to investigate the erosion. In contrast to physical sputtering, arcs produce not only ions and neutral atoms, but also droplets. In a simplified picture arcs are a localised heat source, driven by the ohmic heat of the current in the arc. As the typical spot size is less than a micron, localised melting produces the characteristic traces. Due to the current, arcs have to move in a magnetic field perpendicular to the field direction. The arc jumps from one to another single spot, resulting in the typical arc traces, which can be seen on a macroscopic scale.

Whereas arcing is observed at many tiles in AUG, significant erosion was found only in deposition dominated regions [2]. At the inner baffle region, layers consisting of C, B, W, O and hydrogen isotopes reach a thickness of typical 2-3  $\mu\text{m}$  [5]. Due to the shallow angle of the magnetic field direction and shadowing effects, the thickness of the deposits varies even on one tile. The role of deposits for the arcing process is not completely understood, but it is assumed that the bad electrical conductivity of the deposits reduces the velocity of the arc movement. As the arc burns for a longer time at the same location, it causes stronger erosion.

Local melting and splashing of the molten material, i.e. droplet production, is an important erosion process by arcing. Indeed huge amounts of W droplets are observed in the dust

collected at AUG. Taking the average shot time a flux of  $10^6$  droplets/s with a typical size of 2  $\mu\text{m}$  can be calculated, which results in about 50 % of the dust collected [2].

The erosion by arcing depends on the melting temperature and the heat effusivity of the material used. As the melting temperature of W (3695 K) is much higher than for P92 (1800 K) and the effusivity is also higher (21 vs 9 kW/(m<sup>2</sup>K)) a higher erosion is expected for the steel. Measurements of the erosion rate are mostly from the 80<sup>th</sup> and use a normalisation to the charge of the arcs. Taking the average of different papers [6] a slightly higher erosion of W compared to Fe is expected (78 vs 61  $\mu\text{g}/\text{C}$ ), which is due to the higher specific mass.

## EXPERIMENTAL:

The probes were exposed for one experimental campaign (Dec 13 till Oct 14). They were installed at inner divertor baffle (Bgr.6) of sector 9. After the opening of the vessel the tiles were removed and a part of the probes was cleaned by wiping using deionised water to remove the deposited layers. A confocal laser scanning microscope was used to image the surface by normal optical light microscopy (Fig. 1a and 1c) and to obtain 3D topography data (Fig. 1b and 1d). These 3D data allow determining the material loss. Underneath the deposited layer, a large fraction of the polished surface is unaffected, which is observed at cleaned areas. Any depression beneath the polished surface is assigned as eroded. The volume of these depressions regarding a reference plane parallel to the surface and their areal fraction are shown in Fig. 2.

## TUNGSTEN PROBES:

A view on a typical region of the cleaned W surface is shown in Fig 1a. The polished surface below the deposition layer is partially affected by arcing, the dark structures with the direction from top to bottom. The arcs removed locally the complete deposition layer of typical 3  $\mu\text{m}$  thickness (not shown in this figure). Two different kinds of traces are observed: single craters and complete traces indicating different burning conditions for the arcing. Derived from the optical picture, about 30 % of the surface is affected by arcing, but the depth profile (Fig 1b) is needed to determine the erosion. Most of the traces seen in the optical picture are also found at the depth profile, but the typical erosion is less than 0.2  $\mu\text{m}$ . Additionally, a significant amount of molten W is deposited above the polished level (yellow) close to the erosion region. Only some craters of up to 5  $\mu\text{m}$  depths (blue) are found.

## STEEL PROBES:

An equivalent region as for W is analysed and shown in Fig. 1(c,d) for P92 steel. Again the arcs erode the substrate below the deposition layers. From optical observations about 20 % of the surface is affected by arcing. The number of arc traces is slightly lower than for W. Beside the long arc traces also craters are present (Fig. 1(c)). But in contrast to the W surface the respective craters are much bigger with about 100  $\mu\text{m}$  diameter and about 30  $\mu\text{m}$  depth. These craters dominate the erosion. An interesting detail of the measurements are the direction of the arc traces. As the steel used can be magnetized, the local magnetic field is influenced by the probes themselves. For this reason the direction of the arc traces, which are orientated perpendicular to the magnetic field, bends at the edges of the probes.

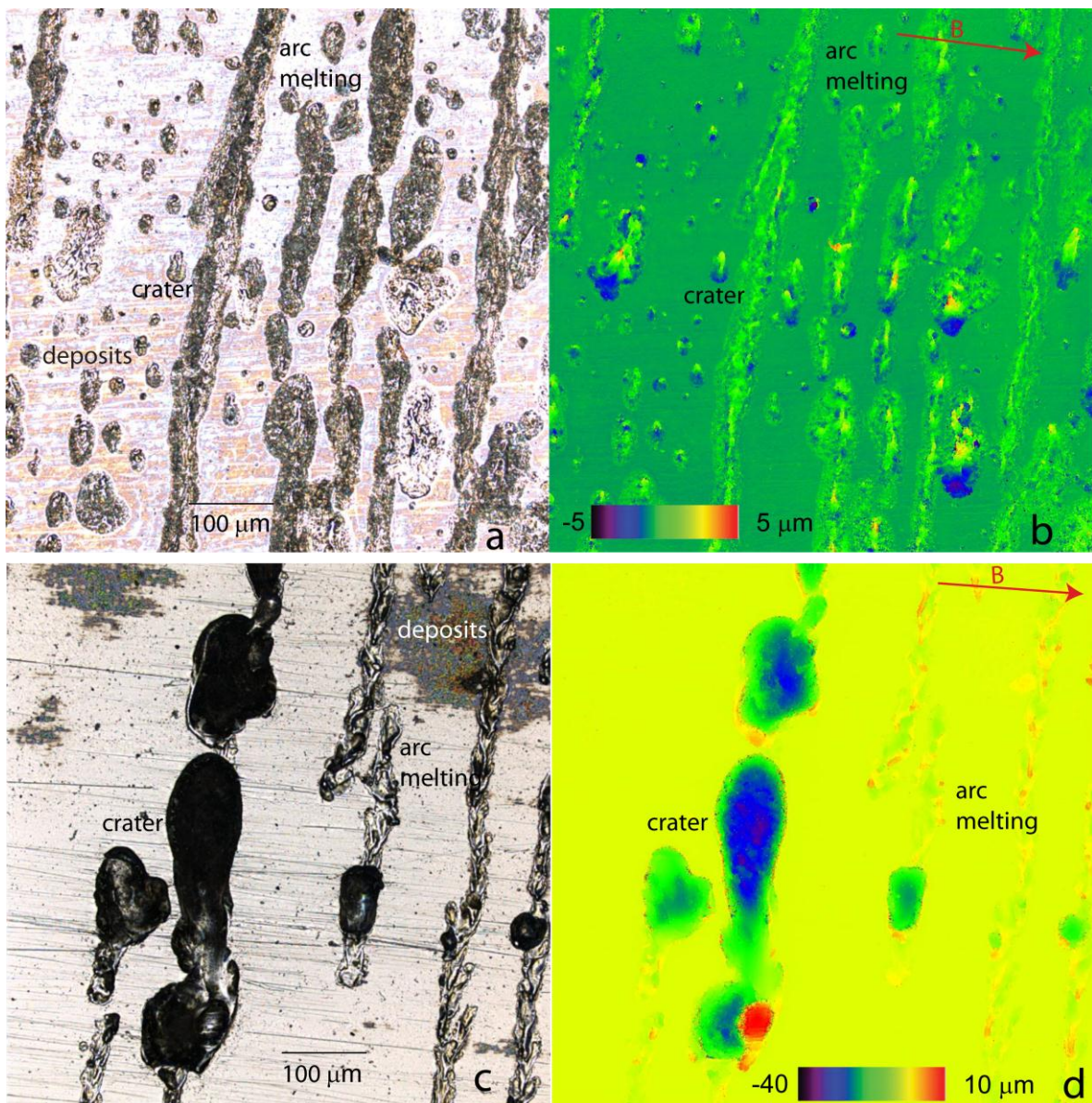


**Figure 1:** Detail of the investigated region showing typical arc traces on W (a, b) and P92 steel (c, d): light microscope images (a, c) and the respective 3D topography data (b, d). The brownish areas in (a, c) are remains from cleaning off the deposited layers. Note the different height scale of the two 3D topography data (b, d).

## DISCUSSION:

To compare the erosion for both materials, depth profiles of a 1.8\*1.8 mm area obtained at the same toroidal and equivalent poloidal positions are used. The volumes of the depressions below a reference plane parallel to the surface were determined for various distances to the surface level. These volumes normalised to the total area analysed, presenting the average erosion, are shown together with the respective area fraction in Fig 2. To measure the total erosion a reference level, presenting the unaffected surface has to be defined. The accuracy of this level is limited by deposits, melting from arcing and the accuracy of the polished surface. To overcome this problem only erosion 0.2  $\mu\text{m}$  below the reference level was taken into account. Using this level only 7.3% of the W surface is eroded by arcing, but 15.6 % of the steel one. Normalizing the total eroded volume to the surface area yields an average erosion of  $\sim 30$  nm for W and  $\sim 920$  nm for P92, i.e. the erosion of steel is 30 times higher compared to

W. The mean erosion rate for the campaign (7125 s of plasma) is  $2.7 \times 10^{13}$  at  $\text{cm}^{-2}\text{s}^{-1}$  for W and  $1.1 \times 10^{15}$  at  $\text{cm}^{-2}\text{s}^{-1}$  for P92. Even as the position of the probes is deposition-dominated, significant erosion is observed, which can be compared with the erosion at the outer divertor strike line of  $7 \times 10^{14}$  at  $\text{cm}^{-2}\text{s}^{-2}$  for W [5].

The big difference of the erosion for W and P92 is not expected from the erosion yield for arcing given in literature [6]. All literature data are for clean surfaces but in AUG the strong erosion is correlated with deposits. The influence of these layers is still not completely understood, and laboratory investigations would be beneficial. A hypothesis to explain the high erosion for P92 is the production of droplets, which increases strongly, as the material temperature reaches the melting point [6]. The lower effusivity and melting temperature for P92 may

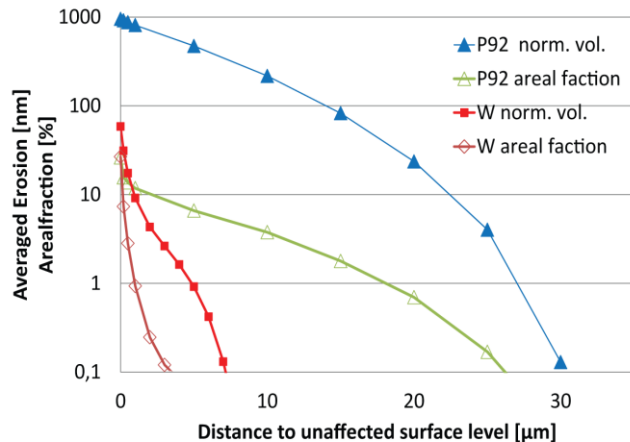


Figure 2: Normalized volume and areal fraction of depression versus distance to the unaffected, originally polished surface.

explain this behaviour. To understand the droplet production, a set of different polished probes was installed for the next experimental campaign of AUG. To scan different melting points and effusivity, this set comprises probes from Al, Cu, Cr, SS, P92, Mo and W.

## CONCLUSION:

At the AUG inner baffle the erosion by arcing on P92 steel is about 30 times higher than for W, i.e. the steel erosion at the baffle region is comparable to W erosion at the outer strike point. Therefore, erosion by arcing has to be taken into account to determine the optimal material mix for future fusion devices. For Be, designed for the inner baffle region of ITER, the melting temperature is close to the steel, but the effusivity is even higher than for W, which complicates predictions. Further investigations, using different materials are started at AUG to disentangle the different effects and to allow estimating the droplet production by arcing.

- [1] McCracken, J.Nucl.Mat., 93, (1980), 3
- [2] Rohde et al., J.Nucl.Mat., 438, (2013), 800
- [3] Balden et al., Nucl.Fusion, 54, (2014), 073010
- [4] Herrmann et al., J.Nucl.Mat., 390, (2009), 747
- [5] Mayer et al., Phys.Scr., T138, (2009), 014039
- [6] Post, Behrisch, Physics of Plasma-Wall interactions in Controlled Fusion, ISBN 0-306-42097-XJ

This work has been carried out within the framework of the EUROfusion Consortium and has received funding from the Euratom research and training programme 2014-2018 under grant agreement No 633053. The views and opinions expressed herein do not necessarily reflect those of the European Commission.